ELSEVIER

Journal of Hydrology 260 (2002) 161–175

Journal of Hydrology

www.elsevier.com/locate/jhydrol

Impact of climate change on water resources in southern Taiwan

Pao-Shan Yu[a,*], Tao-Chang Yang[b], Chih-Kang Wu[a]

[a]*Department of Hydraulics and Ocean Engineering, National Cheng Kung University, Tainan 701, Taiwan, ROC*
[b]*Tainan Hydraulics Laboratory, National Cheng Kung University, Tainan 701, Taiwan, ROC*

Received 27 February 2001; revised 21 August 2001; accepted 17 December 2001

Abstract

This study investigates the impact of climate change on water resources in southern Taiwan. The upstream catchment of Shin-Fa Bridge station in the Kao-Pen Creek basin was the study area chosen herein. The historical trends of meteorological variables, such as mean daily temperature, mean daily precipitation on wet days, monthly wet days, and the transition probabilities of daily precipitation occurrence in each month, at the Kao-Hsiung meteorological station, near the catchments were detected using a non-parametric statistical test. The trends of these meteorological variables were then employed to generate runoff in future climatic conditions using a continuous rainfall–runoff model. The analytical results indicate that the transition probabilities of daily precipitation occurrence significantly influence precipitation generation, and generated runoff for future climatic conditions in southern Taiwan was found to rise during the wet season and decline during the dry season.

Keywords: Climate change; Water resources; Rainfall–runoff model; Transition probability; Trend analysis; Data generation

1. Introduction

Atmospheric carbon dioxide levels have recorded continual increases since the 1950s, a phenomenon that may significantly alter global and local climate characteristics, such as temperature and usable water resources. Tickell (1993) predicted that mean global temperature will increase 1 °C by 2050 and 3 °C by the end of the next century. Meanwhile, in Taiwan, Tsuang et al. (1998) predicted that average temperatures will increase by approximately 0.13 °C per year. The above studies indicate that the global warming has clearly been increasing during recent decades and that the trend may worsen in the future. If the current trend does not change, the impact of global warming on future climatic conditions will become a major concern.

Estimates of global warming are generally based on the application of general circulation models (GCMs), which attempt to predict the impact of increased atmospheric CO_2 concentrations on weather variables. Owing to the complex mechanics at work in the atmosphere and the uncertainty of the model structure, different GCMs produce different predictions. However, despite differing predictions, trends in weather variables were coincident (IPCC, 1990, 1992). Since information on the local or regional impacts of climate change on hydrological processes and water resources over different areas in the world is of great interest, assessing the impact of climate change has recently received extensive attention. Previous studies have usually suggested GCMs coupled with water balance models (Gleick, 1986),

* Corresponding author. Fax: +886-6-2741463.
E-mail address: yups@mail.ncku.edu.tw (P.-S. Yu).

0022-1694/02/$ - see front matter
PII: S0022-1694(01)00614-X

and have generally used these to investigate the impact of climate change on river runoff in different areas (e.g. Cohen, 1986; Gleick, 1987a,b; Bobba et al., 1997; Arnell, 1998; Rosenberg et al., 1999; Najjar, 1999; Mimikou et al., 2000). Furthermore, snowmelt and snow accumulation models have also been combined with soil moisture accounting models using the GCMs results to investigate the impact of climate change (Lettenmaier and Gan, 1990; Panagoulia, 1992). Chang et al. (1992) also thoroughly reviewed pertinent research on how climate change affects water resources. Moreover, many other modelling approaches have been proposed. For example, Burn (1994) examined how climate change affects the timing of the spring runoff event in the west-central region of Canada by using a non-parametric statistical test. Mansell (1997) studied how climate change affects rainfall trends and flood risk in western Scotland by using graphical and basically statistical detection. Westmacott and Burn (1997) evaluated the potential effects of climate change on four hydrologic variables pertaining to the magnitude and timing of hydrologic events within the Churchill-Nelson River basin in west-central Canada by using a non-parametric statistical test. Later, Fowler (1999) assessed potential climate change impacts on water resources in Auckland region (New Zealand) by using climate change scenarios derived in the form of best guesses and envelops. That investigation also proposed a daily water balance model to transform the scenarios into seasonal impacts on the soil water regime and catchments water yield. Seidel et al. (1998) used the high-resolution periodical snow cover mapping by satellites to predict future runoff regimes in an Alpine basin.

For assessing how climate change affects water resources, a more common approach (e.g. Gleick, 1989; Mearns et al., 1990) has been adopted to use primary weather variables such as temperature and precipitation from GCM simulations for the current and doubled atmospheric CO_2 levels. The mean monthly or annual changes in precipitation and temperature are used to modify historical weather records by a fixed quantity determined from a GCM scenario, which then become input data for watershed hydrology models. Such an approach may understate the day-to-day variability of future climatic conditions. An alternative strategy (e.g. Rao and Al-Wagdany, 1995) avoids GCM results entirely and simply changes historic weather variables by some uniform amount before entering them into watershed hydrology models, which may neglect the possibilities of marked change in seasonal climatic patterns produced by global warming. For reflecting possible variations in daily precipitation and daily temperature for future climatic scenarios, Tung and Haith (1995) adopted a weather generating model, including a temperature and a precipitation generating models based on procedures developed by Pickering et al. (1988) and Selker and Haith (1990), to detect global warming effects on New York streamflows by using various GCM results. In our study, this weather-generating model was also adopted, while the parameters of this model are estimated based on the tendencies of historical time series of precipitation and temperature instead of GCM results. The GCMs normally simulate the temperature and precipitation of atmosphere based on the conceptualizations of physics of atmospheric circulation, surface energy, and water fluxes. They must use a spatially coarse grid mesh with a linear scale on the order of hundreds to thousands of kilometers and make simplifications in the modelling processes. Herein, the grid size used in the GCM models is normally significantly larger than Taiwan (i.e. the study area). Downscaling from the GCM results remains a problem, and may cause large errors. The basic assumption of the modelling approach proposed herein is that the tendencies in future precipitation and temperature time series would be the same as in historical precipitation and temperature time series. This assumption differs from the basic assumption in the modelling approach from GCMs, namely that atmospheric levels of CO_2 would double in the future. The model approach used herein takes the historical land surface records into account. The tendency of historical land surface records may result from both global warming and urbanization, which is the true reflection in the study area. Therefore, the modelling approach proposed herein has the advantage of providing decision-makers with the impact of climate change on water resources during a certain period in the future (e.g. 50 or 100 years), unlike the approach of investigating the impact of a doubling in atmospheric CO_2 levels that the decision-makers may not hold the time period of occurrence.

In southern Taiwan, the temporal heterogeneity of

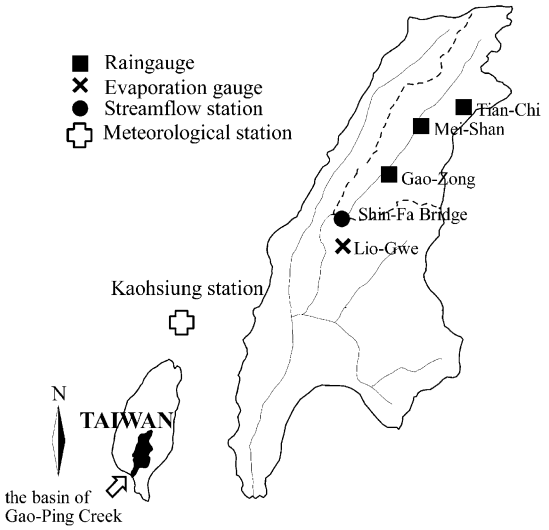

Fig. 1. Locations of the study area and gauged stations.

runoff between high-flow and low-flow periods is obvious, making annual water supply unstable during the year and creating difficulties in water allocation. Therefore, how to preserve runoff during the high-flow period to meet water demand during the low-flow period is an essential issue for southern Taiwan, and the impact of climate change on regional water resources is also a key concern. This study investigates the impact of climate change on water resources in southern Taiwan. Long-term historical data on meteorological variables was gathered first, including mean daily temperature, mean daily precipitation on wet days, monthly wet days, and the monthly transition probabilities of daily precipitation occurrence, to determine the presence and degree of any increasing or decreasing tendencies. A weather-generating model was then constructed to extrapolate future climatic conditions based on the long-term historical tendencies of these meteorological variables. Since trends in the transition probabilities of daily precipitation occurrence may affect the future precipitation generation and yet literature such as Tung and Haith (1995) did not consider this factor, two cases are proposed herein to investigate the difference between results generated with and without considering trends the transition probabilities of daily precipitation occurrence. Finally, the generated future climatic conditions were inputted into a continuous rainfall–runoff model to investigate changes in water resources in southern Taiwan.

2. Description of the study area and data sets

Gao-Ping Creek, is located in southern Taiwan and has the largest catchments on the island, with a drainage area of 3256.85 km^2 and a mainstream length of 171 km. Gao-Ping Creek is the principal water resource in southern Taiwan for agricultural irrigation and water supply. However, the temporal distribution of rainfall throughout the year is strongly heterogeneous. On average, 90% of total annual rainfall falls between May and October in the high-flow period (or the wet season), while November to April of the next year is the low-flow period (or the dry season), with only 10% of annual rainfall. Since the area contains no reservoir, the above weather pattern creates significant difficulties in regional water resource allocation. The Shin-Fa Bridge station is a streamflow stations in the basin of Gao-Ping Creek with no upstream regulation, and has a drainage area of 812.03 km^2. Fig. 1 and Table 1 present and list the locations of the gauged stations used herein, in which rainfall, evaporation, and streamflow stations were used to calibrate the rainfall–runoff model, while

Table 1
The gauged stations used in the study and their record lengths

Station no.	Kinds of observation	Station name	Record length
11P010	Temperature	Kao-Hsiung	1965–1998
11P010	Precipitation	Kao-Hsiung	1932–1998
510031	Streamflow	Shin-Fa Bridge	1961–1992
510129	Precipitation	Gao-Zong	1981–1995
510126	Precipitation	Mei-Shan	1981–1995
510125	Precipitation	Tian-Chi	1981–1995
510014	Evaporation	Lio-Gwe	1981–1995

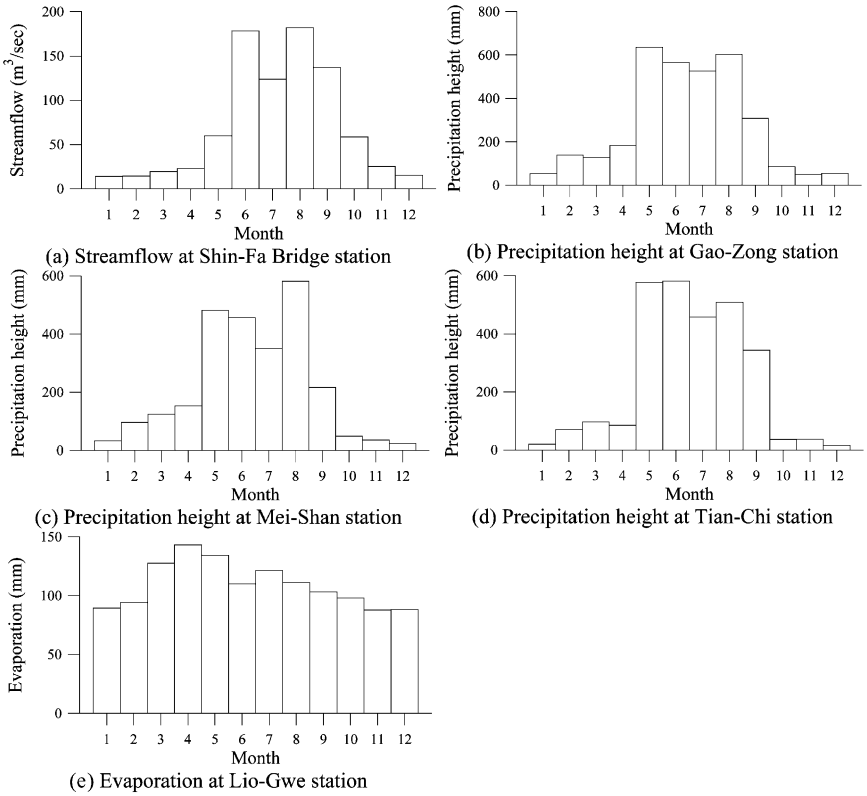

Fig. 2. Average monthly rainfall (mm), evaporation (mm) and streamflow (m^3/s) from the Hydrological Year Book of Taiwan (Water Resources Bureau, 1998).

the Kao-Hsiung meteorological station, which maintained long-term records of daily temperature from 1965 to 1998 and daily precipitation from 1932 to 1998, was used to detect trends in temperature and precipitation. Fig. 2 shows the average monthly rainfall, evaporation, and streamflow in the study area and indicates that rainfall and streamflow are extremely heterogeneous between the wet and dry seasons.

3. Analysis of long-term trends in meteorological variables

Meteorological variables such as temperature and precipitation are found to be highly sensitive in predictions of the effect of climate change on water resources. Consequently, investigating the historical trends of such variables would help to reveal the effects of climate change on water resources. The trend of a time series can be tested using a non-parametric statistical test, Mann–Kendall method (Kendall, 1975), which investigates whether the time series exhibits a significantly increasing or decreasing trend. Herein, four meteorological variables, including mean daily temperature, mean daily precipitation on wet days, monthly wet days, and monthly transition probabilities of daily precipitation occurrence, are used to detect the trends of these four variables. Since readers are familiar with the definitions of the above three meteorological variables, this section merely introduces the definitions of the transition probabilities of daily precipitation occurrence and the Mann–Kendall method, as follows.

3.1. Transition probabilities of daily precipitation occurrence

A first-order two-state Markov chain is used herein

Table 2
The test results of each meteorological variable in each month (*Note*: +, increasing trend; −, decreasing trend, *, indicates no trend; significant level $\alpha = 5\%$)

Month	1	2	3	4	5	6	7	8	9	10	11	12
	Mean value of daily temperature											
Trend	+	+	+	*	+	+	+	+	+	+	+	+
	Mean value of daily precipitation height on wet days											
Trend	+	+	+	+	+	*	*	+	+	−	−	*
	Monthly wet days											
Trend	+	*	*	*	*	−	−	−	−	−	−	−
	Transition probabilities (P_{DD} and P_{WW})											
Trend of P_{DD}	*	*	+	*	*	+	+	+	+	+	*	+
Trend of P_{WW}	+	−	−	−	*	−	−	+	−	−	−	−

to model daily precipitation occurrence, which can be presented by a transition probability matrix comprising four conditional probabilities, as follows:

$$P_{ij} = \begin{bmatrix} P_{D_tD_{t-1}} & P_{W_tD_{t-1}} \\ P_{D_tW_{t-1}} & P_{W_tW_{t-1}} \end{bmatrix} = \begin{bmatrix} P_{D_tD_{t-1}} & 1 - P_{D_tD_{t-1}} \\ 1 - P_{W_tW_{t-1}} & P_{W_tW_{t-1}} \end{bmatrix} \quad (1)$$

where P_{ij} denotes the transition probability matrix of state i given state j, $P_{D_tD_{t-1}}$ (simplified as P_{DD}) represents the conditional probability of a dry day on day t given a dry day on day $(t-1)$, $P_{W_tW_{t-1}}$ (simplified as P_{WW}) is the conditional probability of a wet day on day t given a wet day on day $(t-1)$, $P_{W_tD_{t-1}}$ (simplified as P_{WD}) denotes the conditional probability of a wet day on day t given a dry day on day $(t-1)$, and $P_{D_tW_{t-1}}$ (simplified as P_{DW}) represents the conditional probability of a dry day on day t given a wet day on day $(t-1)$. Estimating the conditional probabilities P_{DD} and P_{WW} allows the entire transition probability matrix to be obtained. Therefore, the conditional probabilities P_{DD} and P_{WW} are selected herein as meteorological variables and their trends determined.

3.2. Mann–Kendall method

The Mann–Kendall method, suggested by the World Meteorological Organization (1988), is a common method of testing the trend of a time series. This method defines the standard normal variate T as:

$$T = \frac{r^*}{\sqrt{\sigma_{2r^*}}} \quad (2)$$

$$r^* = \left[\frac{4p}{n(n-1)}\right] - 1 \quad (3)$$

$$\sigma_{2r^*} = \frac{2(2n+5)}{[9n(n-1)]} \quad (4)$$

where p denotes the number of observation pairs $(x_i, x_j, j > i)$, when $x_j > x_i$ has been calculated and n is the total number of samples. A time series has a clear trend, defined as a level of significance of 5%, if $|T| > T_{\alpha/2} = 1.96$. A positive T indicates an increasing trend in the time series, while a negative T indicates a decreasing trend.

3.3. Test results

Daily temperature data from 1965 to 1998 and daily precipitation data from 1932 to 1998 observed at the Kao-Hsiung station were examined to identify their trends. Mean values of daily temperature and daily precipitation height on wet days, the number of wet days, and the transition probabilities of daily precipitation occurrence (that is, P_{DD} and P_{WW}) were calculated monthly for each year, and trends in the data were then detected using Mann–Kendall method. Table 2 lists the trends that were revealed.

According to this table, the mean daily temperature in each month exhibits a significant increasing trend in every month except April. Meanwhile, the mean values of daily precipitation height display decreasing trends form October to November, no trends at all from June to July and in December, and increasing trends from January to May and August to September. Furthermore, the numbers of wet days exhibit an increasing trend in January, no trends from February to May, and a decreasing

trend from June to December. The values of P_{DD} exhibit an increasing trend in March, from June to October, and in December, and have no trend at all from January to February and April to May. Finally, the values of P_{WW} reveal an increasing trend from January and August, no trend in May, and decreasing trends from February to April, June to July, and September to December. The above measured results reveal that in most months the mean values of daily temperature and precipitation height on wet days exhibit increasing tendencies, while the opposite is true for monthly wet days. The transition probabilities of daily precipitation occurrence, P_{DD} and P_{WW}, display significant trends in most months, revealing changing rainfall patterns during the historical period sampled herein.

4. Weather generating model

Weather generating records were selected to reflect possible variations in daily temperatures and precipitation heights. The generation algorithms were based on procedures developed by Pickering et al. (1988) and Selker and Haith (1990). Daily temperatures were calculated by the first-order autoregressive equation presented in Pickering et al. (1988). For generating daily precipitation heights, a Markov chain was first used to determine the occurrence of wet and dry days. Daily precipitation height on wet days was then determined by sampling from the Weibull distribution. The temperature and precipitation generating models are detailed further below.

4.1. Temperature generating model

A first-order autoregressive model was utilized to generate daily temperature sequences, with the following form:

$$t_k = \mu_T + \rho_{1T}(t_{k-1} - \mu_T) + \sqrt{1 - \rho_{1T}^2}\sigma_T v_k \tag{5}$$

where t_k denotes the temperature on day k, μ_T represents the mean temperature for a period (1 month herein), σ_T is the standard deviation of temperature during that period, ρ_{1T} denotes the lag-one autocorrelation coefficient of temperature during that period, and v_k represents the random standard normal variate. Given the parameters, μ_T, σ_T, and ρ_{1T}, a daily temperature sequence can be generated using this model.

To generate the daily temperature sequence of future climatic conditions, three parameters of future climatic conditions must be determined, namely, $\mu_{T_{i,j}}$, $\sigma_{T_{i,j}}$, and $\rho_{1T_{i,j}}$, where $\mu_{T_{i,j}}$ denotes the mean temperature for month j in year i, $\sigma_{T_{i,j}}$ represents the standard deviation of the temperature for month j in year i, and $\rho_{1T_{i,j}}$ is the lag-one autocorrelation coefficient of the temperature for month j in year i.

Herein, the trends of mean monthly temperature and mean monthly precipitation were determined using not only the Mann–Kendall test but also linear regression analysis. The test results revealed that in most months the series could pass the F-test, and thus the series clearly contain linear components. After separating the linear components, series vibration can be simulated by using the stochastic component. A linear regression equation (linear component) combined with a first-order autoregressive model (stochastic component) was developed to calculate the future value of $\mu_{T_{i,j}}$, as follows:

$$\mu_{T_{i,j}} = S_{T_j} \times (i - y_0) + \bar{\mu}'_{T_j} + \rho'_{T_j} \cdot \frac{\sigma'_{T_j}}{\sigma'_{T_{j-1}}} \cdot (\mu_{T_{i,j-1}} - \bar{\mu}'_{T_j}) + \sqrt{1 - \rho'^2_{T_j}}\sigma'_{T_j} \nu_{i,j} \tag{6}$$

where S_{T_j} denotes the coefficient of the linear regression equation relating mean temperature in month j to time (year), $\bar{\mu}'_{T_j}$ represents the mean value of mean temperature in month j, σ'_{T_j} is the standard deviation of mean temperature in month j, ρ'_{T_j} denotes the autocorrelation coefficient of mean temperature values between months j and $j-1$, y_0 represents the initial year of generation, and $\nu_{i,j}$ is the random standard normal variate. The former four parameters are calculated using the data during the current climatic period.

Since the mean values and standard deviations of temperature for all months were found to correlate strongly, this study attempted to establish the relationship between historical mean temperatures, μ_T, and standard deviations, σ_T, for all months by a linear regression equation, as follows:

$$\sigma_T = -0.14358 \times \mu_T + 5.16122, \quad \text{Correlation coefficient} = 0.73 \tag{7}$$

After obtaining the mean monthly temperature for future climatic conditions, the standard deviation of

Table 3
The lag-one autocorrelation coefficient of temperature for each month

Month	1	2	3	4	5	6	7	8	9	10	11	12
Value	0.67	0.71	0.71	0.68	0.66	0.7	0.61	0.57	0.68	0.74	0.75	0.73

monthly temperature for future climatic conditions can be obtained by substituting the mean temperature into the above regression equation. The lag-one autocorrelation coefficient of temperature for future climatic conditions for month j in year i, $\rho_{1T_{i,j}}$, was considered herein to be the same as that of current climatic conditions. Table 3 lists the lag-one autocorrelation coefficients of temperature for all months, calculated using the data during the current climatic period.

To validate the above temperature generating model, parameters, μ_T, σ_T, and ρ_{1T} from Eq. (5) were obtained for each month by using historical daily temperature records during the period from 1965 to 1998 at Kao-Hsiung station, and 50 sets of daily temperature sequences with the same period were generated to determine whether the first two statistical moments of daily temperature for each month could be preserved. Fig. 3 compares the mean temperature and standard deviation generated for each month with the observed values, and reveals that the temperature generating model achieves good validation results. These good validation results also implicitly justify the assumptions of the temperature generating model, such as the form of Eq. (5) and the probabilistic distribution of daily temperature values.

4.2. Precipitation generating model

For generating daily precipitation heights, a first-order two-state Markov chain was selected to model daily precipitation occurrence of wet and dry days. Combining the Markov chain and the probabilistic distribution of precipitation height on a wet day produces the overall probability distribution for precipitation height. Though various probabilistic distributions have been considered for wet-day precipitation height (Pickering et al., 1988; Selker and Haith, 1990), the two more commonly used distributions, that is, the exponential distribution and the Weibull distribution, were adopted herein to test their suitability to the study area, and the Weibull distribution was found to be superior to the exponential distribution. Meanwhile, if the occurrence of wet days can be determined by the Markov chain, the precipitation heights can be estimated by the Weibull distribution. The Weibull distribution takes the following form:

$$p_t = \alpha \exp\left\{-\frac{1}{\beta}\cdot\ln[\ln(1-u_t)]\right\} \tag{8}$$

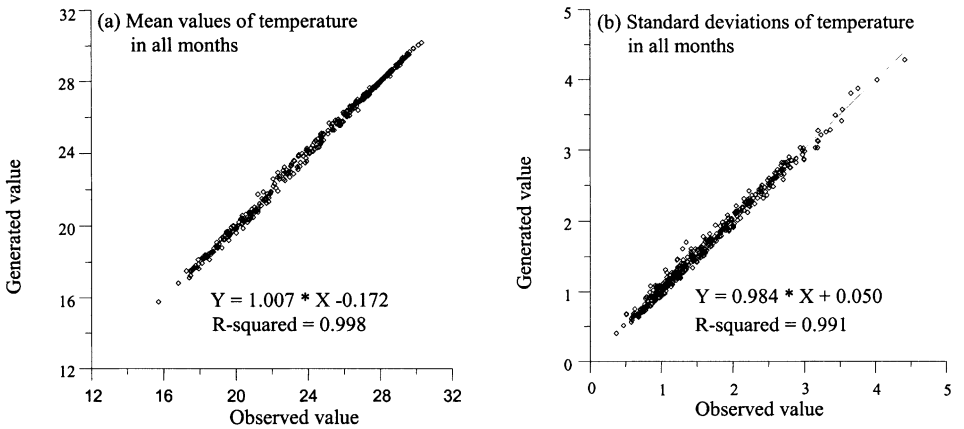

Fig. 3. Validation results of the temperature generating model.

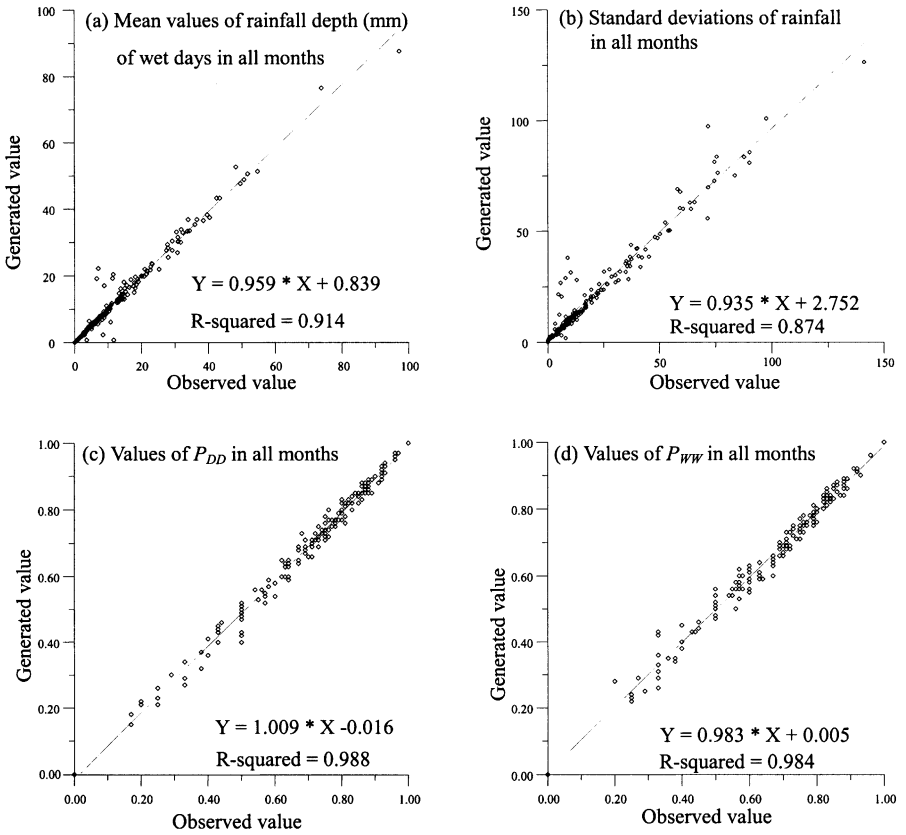

Fig. 4. Validation results of the precipitation generating model.

where p_t denotes the precipitation height on day t, u_t represents the random variable between 0 and 1, and α and β are the parameters of the Weibull distribution, which can be estimated using the mean precipitation height, μ_p, and the standard deviation of precipitation, σ_p. Therefore, the daily precipitation height sequences can be generated based on the following six parameters: mean precipitation height in a period, μ_p, the standard deviation of precipitation in that period, σ_p, and the transition probabilities of daily precipitation occurrence (P_{DD}, P_{DW}, P_{WD}, and P_{WW}).

To generate the daily precipitation height sequences of future climatic conditions, the values of the above six parameters must be predicted. Herein, the mean precipitation height for month j in year i for future climatic conditions, $\mu_{p_{i,j}}$, is determined by an equation similar in form to Eq. (6), where temperature is modified by precipitation.

To obtain the standard deviation of precipitation height for month j in year i, $\sigma_{p_{i,j}}$, for future climatic conditions, the historical mean values, μ_p, were related to the standard deviations of precipitation height, σ_p, for all months, revealing a high correlation coefficient, as follows:

$$\sigma_p = 1.61116 \times \mu_p - 1.52341, \quad \text{Correlation coefficient} = 0.94 \tag{9}$$

The standard deviation of precipitation height for future climatic conditions can be calculated by substituting the generated mean precipitation height of future climatic conditions into this equation.

This study first utilized a linear equation to extrapolate the mean tendency of the transition probabilities of daily precipitation occurrence ($P_{\mathrm{DD}_{i,j}}$, $P_{\mathrm{WD}_{i,j}}$, $P_{\mathrm{DW}_{i,j}}$, and $P_{\mathrm{WW}_{i,j}}$) of future climatic conditions for

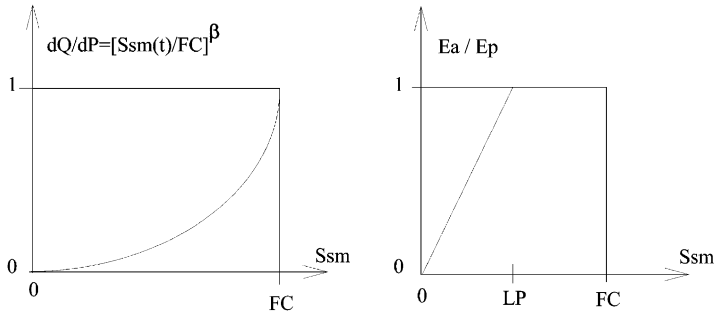

Fig. 5. Schematic presentation of the soil moisture and evapotranspiration relation in the HBV model.

month j in year i. The equations were constructed as follows:

$$P_{\mathrm{DD}_{i,j}} = \mu'_{P_{\mathrm{DD}_j}} + S_{P_{\mathrm{DD}_j}} \times (i - y_0) \tag{10}$$

$$P_{\mathrm{WD}_{i,j}} = 1 - P_{\mathrm{DD}_{i,j}} \tag{11}$$

$$P_{\mathrm{WW}_{i,j}} = \mu'_{P_{\mathrm{WW}_j}} + S_{P_{\mathrm{WW}_j}} \times (i - y_0) \tag{12}$$

$$P_{\mathrm{DW}_{i,j}} = 1 - P_{\mathrm{WW}_{i,j}} \tag{13}$$

where $\mu'_{P_{\mathrm{DD}_j}}$ and $\mu'_{P_{\mathrm{WW}_j}}$ denote the mean values of the transition probabilities P_{DD} and P_{WW}, respectively, in month j, as calculated from current climatic conditions; y_0 represents the initial year of generation; and $S_{P_{\mathrm{DD}_j}}$ and $S_{P_{\mathrm{WW}_j}}$ are the coefficients of the regression equations for month j that relate transition probabilities P_{DD} and P_{WW}, respectively, with time (year) for current climatic conditions.

To validate the above precipitation generating model, parameters, μ_p, σ_p, P_{DD}, and P_{WW} were obtained for each month from daily areal precipitation height records, as estimated from the precipitation records of the three raingauges (namely, the Gao-Zong, Mei-Shan, Tian-Chi stations listed in Table 1) using Thiessen weights during the period from 1981 to1995. Fifty sets of daily precipitation height sequences with the same period were generated to determine whether the values of μ_p, σ_p, P_{DD}, and P_{WW} generated in each month could be preserved as well as the observed values. Fig. 4 compares the generated values of μ_p, σ_p, P_{DD} and P_{WW} for all months with the observed ones, revealing that the precipitation generating model has good validation results. These good validation results also implicitly justify the assumptions of the precipitation height generating model, such as the form of the probabilistic distribution of daily precipitation heights.

5. Rainfall–runoff model structure and calibrated parameters

Designed by the Swedish Meteorological and Hydrological Institute, the HBV hydrological model has been successfully applied in more than 30 countries (Bergström, 1976, 1992; Bathia et al., 1984; Häggström et al., 1990), which is adopted in our study.

Fig. 5 displays the soil moisture routine. β controls the contribution ($\mathrm{d}Q$) to the runoff response routing and the increase ($\mathrm{d}P - \mathrm{d}Q$) in soil moisture storage (Ssm). Meanwhile, FC denotes the maximum Ssm in the model. The relationship among the above parameters is given by $\mathrm{d}Q/\mathrm{d}P = (\mathrm{Ssm}/\mathrm{FC})^{\beta}$, where P denotes precipitation. LP represents the value of the soil moisture, above which evapotranspiration (Ea) reaches its potential limit (E_{p}). Since mass balance over the soil is given by: $\mathrm{d}Q = \mathrm{d}P - \mathrm{dSsm}$, soil moisture accounting can be expressed as $\mathrm{dSsm}/\mathrm{d}P = 1 - (\mathrm{Ssm}/\mathrm{FC})^{\beta}$.

The runoff response routine includes two tanks (Fig. 6) that distribute the generated runoff in time, so that the quick and slow parts of the recession are obtained. The lower tank storage (Slz) is filled by percolation from the upper tank (PERC), and K_2 is the recession coefficient. If the yield ($\mathrm{d}Q$) from the soil moisture routine exceeds the capacity, the upper tank will start to fill. Upper tank storage (Suz) is drained by two recession coefficients, K_0 and K_1,

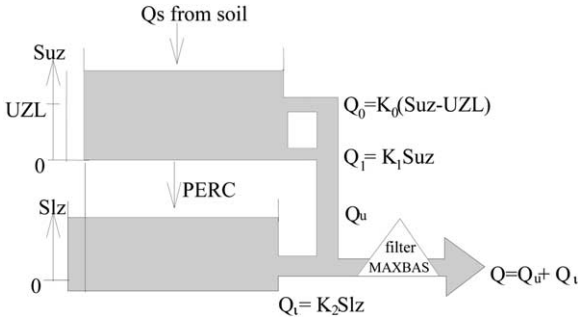

Fig. 6. The runoff-response function of the HBV model.

separated by a threshold (UZL). This tank models the response during floods. A simple routing transformation is made to account for the damping of the flood pulse in the river before it reaches the basin outlet. This filter has a triangular distribution of weights with the base length, MAXBAS. Zhang and Lindström (1997) slightly modified the model structure by introducing a new parameter, Ce, into the soil moisture routine. This parameter, Ce, was multiplied with the potential evapotranspiration and also adopted herein.

For model calibration, the HBV model was applied to the upstream catchments of the Shin-Fa Bridge station to explore its ability to simulate streamflow. The objective function, FMOF (Yu and Yang, 2000), and shuffled complex evolution (SCE) optimization method (Duan et al., 1992, 1993, 1994) were used herein. The streamflow records at the Shin-Fa Bridge station were divided into the calibration period (1981–1990) and verification period (1991–1992). Table 1 lists the rain and evaporation gauges used for this catchments, while Table 4 lists the calibrated values of the model parameters. Fig. 7 displays the performances of the streamflows simulated in the verification period (1991–1992) by plotting the simulated and observed hydrographs, and by calculating the Nash–Sutcliffe statistics, revealing that the model can accurately simulate the historical flow series.

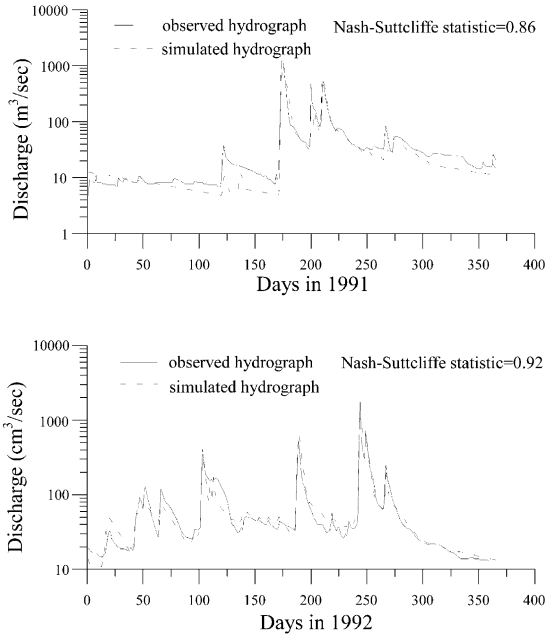

Fig. 7. The simulated and observed hydrographs in the verification period (1991–1992).

6. Impact of global warming on water resources

Besides considering the temperature trends, this study detects two climate change scenarios that make different assumptions regarding the occurrence of precipitation: Case 1 considers trends in the transition probabilities of daily precipitation occurrence, while Case 2 does not. By using the weather generating model, 50 sets of future weather sequences (for 2000–2050) are generated using each case, including daily temperature and precipitation height sequences. Table 5 lists the estimated coefficients of the regression equations in different months that relate mean temperature, mean precipitation, and transition probabilities (P_{DD} and P_{WW}), respectively, against time (year) for current climatic conditions. The information from the table was used in Section 4 to generate

Table 4
The calibrated values of model parameters

	FC	β	LP	PERC	UZL	K_0	K_1	K_2	Ce
Value	198.458	8.288	81.368	2.566	152.624	0.214	0.044	0.008	0.495
Unit	mm	–	mm	mm	mm	day^{-1}	day^{-1}	day^{-1}	–

Table 5
The coefficients of the regression equations in different months relating mean temperature, mean precipitation, and transition probabilities (P_{DD} and P_{WW}), respectively, against time (year) for current climatic conditions

Month j	S_{T_j}	S_{P_j}	$S_{P_{DD_j}}$	$S_{P_{WW_j}}$
1	0.0554	0.0347	−0.00014	0.00255
2	0.0461	0.0329	−0.00034	−0.00121
3	0.0431	0.0484	0.00115	−0.00118
4	0.0194	0.0635	0.00031	−0.00194
5	0.0166	0.1277	−0.00006	−0.00033
6	0.0448	0.0076	0.00145	−0.00108
7	0.0474	−0.0051	0.00290	−0.00188
8	0.0509	0.0482	0.00114	0.00092
9	0.0291	0.1521	0.00143	−0.00070
10	0.0395	−0.0784	0.00047	−0.00329
11	0.0609	−0.0501	0.00010	−0.00234

the parameters of the model for generating future weather (for 2000–2050). Fig. 8 shows the generated mean temperature and mean precipitation height on wet days after it was averaged by 50 sets of weather sequences from March for Case 1 for the future years (2000–2050). The figure reveals that this weather generating model may reflect possible variations and trends in daily temperature and precipitation for future climatic scenarios. Fig. 9 compares annual generated precipitation heights for cases 1 and 2 from 2000 to 2050, and reveals that the values of Case 1 are lower than those of Case 2. Accordingly, it appears that the precipitation heights generated for future climatic scenarios where the transition probabilities of precipitation occurrence are not considered might be overestimated.

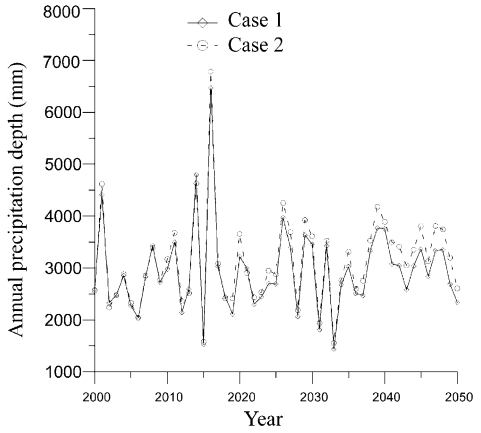

Fig. 9. Generated annual precipitation heights for Case 1 and Case 2, respectively, in the future years.

After generating the daily temperature series for future climatic scenarios, Hamon's (1961) temperature-dependent equation was used to transform the daily temperature series into the daily evapotranspiration series. Hamon's temperature-dependent equation is expressed as:

$$E_p(t) = 0.021H(t)^2 e_0(t)/[T(t) + 273] \quad (14)$$

where $E_p(t)$ denotes evapotranspiration (cm/day) on day t; $H(t)$ represents sunshine hours on day t; $e_0(t)$ is the saturated vapor pressure (milibar) on day t; and $T(t)$ denotes mean temperature (°C) on day t. $H(t)$ was taken from the Kao-Hsiung meteorological station and $e_0(t)$ can estimated by the following empirical

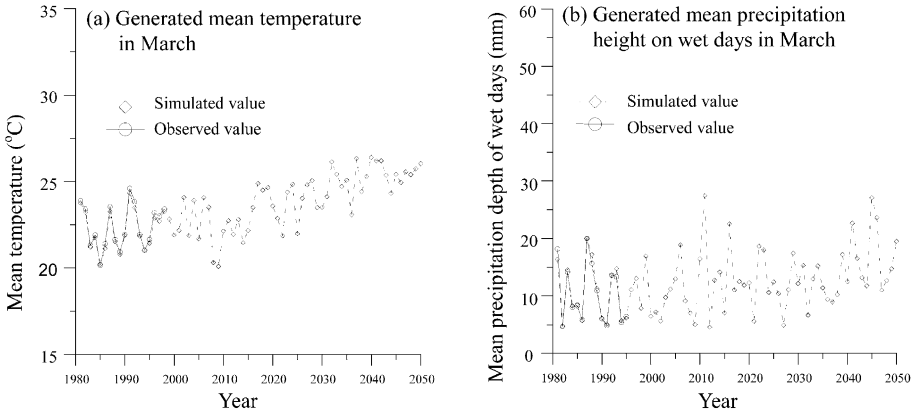

Fig. 8. Generated mean temperature and mean precipitation height on wet days in March for the future years.

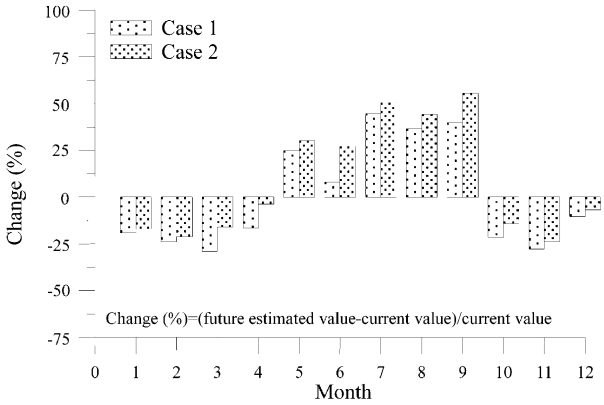

Fig. 10. Comparisons of mean values of daily runoff for all months between the current climatic condition and the future climatic conditions (cases1 and 2).

equation.

$$e_0(t) = 33.8639[(0.00738 \times T(t) + 0.8072)8 - 0.000019 \times |1.8 \cdot T(t) + 48| + 0.001316] \quad (15)$$

The generated daily precipitation height series and evapotranspiration series were than inputted into the HBV model to simulate the flow series for future climatic conditions. The following sections compare (1) mean values of daily flow for all months, (2) runoff volumes during the high-flow and low-flow periods, (3) annual mean daily flows, (4) discharges of 95% exceeding percentage, and (5) mean values of annual maximum 1-day flow between the current and future climatic conditions (including cases 1 and 2).

The observed flow series from 1961 to 1992 were adopted as the current climatic condition, while the 50 sets of flows from 2000 to 2050 generated by the weather-generating and HBV models were used to represent future climatic conditions. Furthermore, mean values of daily flow are calculated every month for the current and future climatic conditions. Meanwhile, the percentage changes of these calculated values for the future climatic conditions to the current climatic condition were estimated to determine the impact of climate change, as shown in Fig. 10. This figure clearly indicates that runoff increases from May to September, and that the percentage change is smaller in Case 1 than in Case 2. Runoff decreases from October to April the following year, and with the decrease being greater in Case 1 than in Case 2.

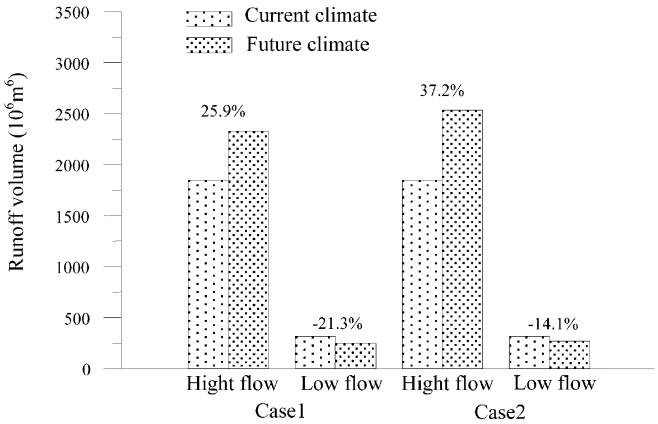

Fig. 11. Runoff volumes influenced by climatic change during the high-flow and low-flow periods for cases 1 and 2.

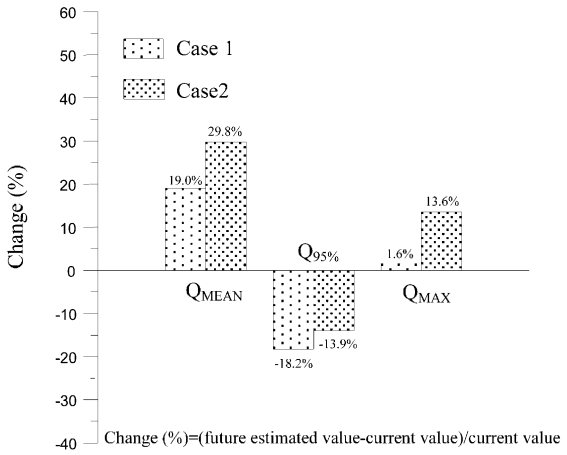

Fig. 12. The change percentages of Q_{MEAN}, Q_{MAX}, and $Q_{95\%}$ influenced by climatic change for cases 1 and 2.

To get another picture of likely variations in water resources during the wet and dry seasons, runoff volumes are calculated during the high-flow period (May to October) and low-flow period (November to April of the next year). As shown in Fig. 11, the runoff volume of the high-flow period increases 25.9% for Case 1 and 37.2% for Case 2, and the runoff volume during the low-flow period may decrease 21.3% for Case 1 and 14.1% for Case 2. The temporal heterogeneity of runoff might increase in the future, warning of potential problems in water resource allocation given the lack of reservoirs in the region. If the trends in transition probabilities are taken into account (Case 1), the increases in runoff volume are less than without such trends (Case 2).

To further compare how climate change affected river flows, annual mean daily flows (Q_{MEAN}), discharges of 95% exceeding percentage ($Q_{95\%}$), and mean values of annual maximum 1-day flow (Q_{MAX}) for current and future climatic conditions (i.e. cases 1 and 2) were estimated. Fig. 12 shows the percentage changes for future climatic conditions (namely, cases 1 and 2) to the current climatic condition. The figure reveals that the Q_{MEAN} and Q_{MAX} increase for the future climatic condition, and that the percentage change in Case 1 is smaller than that in Case 2. Meanwhile, $Q_{95\%}$ decreases for the future climatic condition, and the percentage change in Case 1 is larger than that in Case 2. The figure also displays these values of percentage changes.

Based on the above analyses, it is concluded that the trends of the transition probabilities of daily precipitation occurrence significantly influence the future variation of water resources, and failing to consider the transition probabilities of daily precipitation occurrence (Case 2) may overestimate runoff compared to when the transition probabilities of daily precipitation occurrence (Case 1) are considered.

7. Conclusions

This study investigated the impact of climate change on water resources in the Kao-Pen Creek basin, southern Taiwan. The upstream catchment of Shin-Fa Bridge station in the Kao-Pen Creek basin was selected for study herein.

First, the Mann–Kendall method was adopted to identify long-term precipitation and temperature trends at the Kao-Hsiung meteorological station. The analytical results indicate that the temperature increases over the long-term period and the transition probabilities of daily precipitation occurrence change significantly, two results that were used to generate weather series for future climatic conditions based on the theory of Thomas-Fiering. Temperature was found herein to follow a clear and steady trend every month. The mean values of precipitation height on wet days exhibit increasing trends from January to May (low-flow period), while monthly wet days decrease from June to December (high-flow period). Meanwhile, for many months, the transition probabilities of dry day to dry day increase, while those of wet day to wet day decrease. This phenomenon reveals a clear change in rainfall type. Furthermore, the intensity of future precipitation may increase owing to increasing height and decreasing duration.

Finally, the generated weather series (i.e. temperature and precipitation height) for future climatic conditions were inputted into a continuous rainfall–runoff model to investigate the changes in water resources. The results from the study area indicate that future runoff displays an increasing tendency during the wet season, and tends to decrease during the dry season. Additionally, when the trends of the transition probabilities of daily precipitation occurrence are considered, the impacts of climate change

on water resources differ from when no trends in the transition probabilities of daily precipitation occurrence are considered. If no trends in the transition probabilities of daily precipitation occurrence are considered, runoff for the future climatic condition would be overestimated. Moreover, the increase of runoff for the future climatic condition would be 26% of the runoff volume for the current climatic condition during the high-flow period (May to October) and the decrease of runoff would be 21% during the low-flow period (November to April of the next year) during a 50-year period (2000–2050). Such a trend would highlight the difference in runoff between the high-flow and low-flow periods. Future water resources allocations, particularly for the south Taiwan region, which has relatively few reservoirs, may become increasingly challenging due to the growing variation of runoff between the high-flow and low-flow periods. How to more efficiently reserve runoff during the high-flow period for water demand during the low-flow period will become an essential future issue for this region.

Readers should be aware of some issues regarding the length of data records and assumptions of models used herein. Indeed, the length of data records is an essential influence on the results of trend analysis and on projected changes in runoff. The results of runoff simulation for the future climatic condition could be influenced if the trends over a longer time period indicated a different rate of change in the meteorological variables. The time period of the data used herein for tendency analysis spans over 30 years (daily temperature data from 1965 to 1998 and daily precipitation data from 1932 to 1998). The processes of global warming and urbanization have presumably been particularly strong during recent years, thus it is supposed that the data sample period used herein should be sufficient to reflect the major historical changes. Questions such as whether a longer sample period would be useful of necessary, and the length of the data analyzed herein are interesting topics which will be studied in future works.

The trend of increasing temperature noted herein may not be entirely caused by global warming, despite accurately reflecting local climate change. Though the increasing temperature trend may be a combination of the results of global warming and urbanization, distinguishing between the effects of global warming and urbanization in a local area is difficult. Therefore, this work merely assumes the increasing temperature to indicate local climate change, leaving the possibility of a connection with global warming to be investigated by a future study.

In the present stage of this study, owing to the difficulty of constructing a model for extrapolating the serial correlation of temperature values in the future and the scarcity of literature on this issue, the serial correlation was assumed herein to remain constant over time, which needs more explorations. This study only focused on the mean tendency of the transition probabilities of precipitation occurrence, investigating the influence of this tendency on streamflow. Therefore, the linear trends in Eqs. (10)–(13) were adopted in this preliminary investigation, which should be studied in more detail in a future work.

Acknowledgements

The authors would like to thank the National Science Council, Republic of China for financially supporting this research under Contract No. NSC89-2211-E006-066. The reviewers are also appreciated for their valuable comments.

References

Arnell, N.W., 1998. Climate change and water resources in Britain. Climatic Change 39 (1), 83–110.

Bathia, P.K., Bergström, S., Person, M., 1984. Application of the distributed HBV-6 model to the upper Narmada Basin in India, Report RHO 35, Swedish Meteorological and Hydrological Institute, Norrköping, Sweden.

Bergström, S., 1976. Development and application of a conceptual runoff model for Scandinavian catchments, Report RHO 7, Swedish Meteorological and Hydrological Institute, Norrköping, Sweden.

Bergström, S., 1992. The HBV model-its structure and applications, SMHI Report Hydro., RH No. 4, Swedish Meteorological and Hydrological Institute, Norrköping, Sweden.

Bobba, A.G., Singh, V.P., Jeffries, D.S., Bengtsson, L., 1997. Application of a watershed runoff model to north-east pond river, Newfoundland: to study water balance and hydrological characteristics owing to atmospheric change. Hydrological processes 11 (12), 1573–1593.

Burn, D.H., 1994. Hydrologic effects of climatic change in the west-central Canada. Journal of Hydrology 160, 53–70.

Chang, L.H., Hunsaker, C.T., Draves, J.D., 1992. Recent research

on effects of climate change on water resources. Water Resource Bulletin 28 (2), 273–286.

Cohen, S.J., 1986. Impacts of CO_2-induced climatic change on water resources in the Great Lakes basin. Climate Change 8, 135–153.

Duan, Q., Sorooshian, S., Gupta, V.K., 1992. Effective and efficient global optimisation for conceptual rainfall–runoff models. Water Resources Research 28 (4), 1015–1031.

Duan, Q., Gupta, V.K., Sorooshian, S., 1993. A shuffled complex evolution approach for effective and efficient global minimization. Journal of Optimisation Theory and Applications 76 (3), 501–521.

Duan, Q., Sorooshian, S., Gupta, V.K., 1994. Optimal use of the SCE-UA global optimisation method for calibrating watershed models. Journal of Hydrology 158, 265–284.

Fowler, A., 1999. Potential climate change impacts on water resources in the Auckland Region (New Zealand). Climate Research 11 (3), 221–245.

Gleick, P.H., 1986. Methods for evaluating the regional hydrologic impacts of global climatic change. Journal of Hydrology 88, 97–116.

Gleick, P.H., 1987a. The development and testing of a water balance model for climate impacts assessment: modelling the Sacramento basin. Water Resource Research 23 (6), 1049–1061.

Gleick, P.H., 1987b. Regional hydrologic consequences of increases in atmospheric CO_2 and other trace gases. Climatic Change 10, 137–161.

Gleick, P.H., 1989. Climate change, hydrology, and water resources. Review of Geophysics 27 (3), 329–344.

Häggström, M., Lindström, G., Cobos, C., Martinez, J.R., Merlos, L., Alonzo, R.D., Castillo, G., Sirias, C., Miranda, D., Granados, J.I., Alfaro, R.I., Robles, E., Rodriguez, M., Moscote, R., 1990. Application of the HBV Model for Flood Forecasting in Six Central American Rivers. Swedish Meteorological and Hydrological Institute, Norrköping, Sweden 73 pp..

Hamon, W.R., 1961. Estimating potential evapotranspiration. Journal of Hydraulics Division 87(3), 107–120.

IPCC (Intergovernmental Panel on Climate Change), 1990. In: Houghton, J.T., Jenkins, G.J., Ephraums, J.J. (Eds.). Climate Change: The IPCC Scientific Assessment. Cambridge University Press, Cambridge, UK 365 pp..

IPCC (Intergovernmental Panel on Climate Change), 1992. In: Houghton, J.T., Callander, B.A., Varney, S.K. (Eds.). Climate Change 1992, the Supplementary 1992: Report to the IPCC Scientific Assessment. Cambridge University Press, Cambridge, UK 200 pp..

Kendall, M.G., 1975. Rank Correlation Measures. Charles Griffin, London p. 220.

Lettenmaier, D.P., Gan, T.Y., 1990. Hydrologic sensitivities of the Sacramento–San Joaquin river basin, California, to global warming. Water Resources Research 26 (1), 69–86.

Mansell, M.G., 1997. The effect of climate change on rainfall trends and flood risk in the west of Scotland. Nordic Hydrology 28, 37–50.

Mearns, L.O., Gleick, P.H., Schneider, S.H., 1990. Climate forecasting. In: Waggoner, P.E. (Ed.). Climate Change and U.S. Water Resources. Wiley, New York, NY.

Mimikou, M.A., Baltas, E., Varanou, E., Pantazis, K., 2000. Regional impacts of climate change on water resources quantity and quality indicators. Journal of Hydrology 234, 95–109.

Najjar, R.G., 1999. The water balance of the Susquehanna River Basin and its response to climate change. Journal of Hydrology 219, 7–19.

Panagoulia, D., 1992. Impacts of GISS-modelled climate changes on catchment hydrology. Hydrological Sciences Journal 37 (2), 141–163.

Pickering, N.B., Stedinger, J.R., Haith, D.A., 1988. Weather input for nonpoint source pollution models. Journal of Irrigation and Drainage Engineering 114 (4), 674–690.

Rao, A.R., Al-Wagdany, A., 1995. Effects of climatic change in Wabash river basin. Journal of Irrigation and Drainage Engineering 121 (2), 207–215.

Rosenberg, N.J., Epstein, D.J., Wang, D., Vail, L., Srinivasan, R., Arnold, J.G., 1999. Possible impacts of global warming on the hydrology of the Ogallala aquifer region. Climatic Change 42 (4), 677–692.

Seidel, K., Ehrler, C., Martinec, J., 1998. Effects of climate change on water resources and runoff in an Alpine basin. Hydrological Processes 12, 1659–1669.

Selker, J.S., Haith, D.A., 1990. Development and testing of single-parameter precipitation distributions. Water Resource Research 26 (11), 2733–2740.

Tickell, C., 1993. Global warming and its effects. Engineering for Climate Change. Institute of Civil Engineers, UK, pp. 9–16.

Tsuang, B.J., Wu, M.C., Liu, C.C., Chen, H.H., 1998. Climatic change and prediction in Taiwan. Journal of Nature 58, 106–112 in Chinese.

Tung, C.P., Haith, D.A., 1995. Global-warming effects on New York streamflows. Journal of Water Resources Planning and Management 121 (2), 216–225.

Water Resources Bureau, 1998. Hydrological Year Book of Taiwan 1997. Ministry of Economic Affairs, Taiwan, ROC.

Westmacott, J.R., Burn, D.H., 1997. Climate change effects on the hydrologic regime within the Churchill-Nelson River Basin. Journal of Hydrology 202, 263–279.

World Meteorological Organization, 1988. Analyzing long time series of hydrological data with respect to climate variability, Wcap-3, WMO/TD 224.

Yu, P.S., Yang, T.C., 2000. Fuzzy multi-objective function for rainfall–runoff model calibration. Journal of Hydrology 238, 1–14.

Zhang, X., Lindström, G., 1997. Developed of an automatic calibration scheme for the HBV model. Hydrological Processes 11, 1671–1682.